

## 6.9 A CMOS Electrochemical Impedance Spectroscopy Biosensor Array for Label-Free Biomolecular Detection

Arun Manickam, Aaron Chevalier, Mark McDermott, Andrew D Ellington, Arjang Hassibi

University of Texas, Austin, TX

Biosensors are one of the fundamental detection platforms in biotechnology. They take advantage of unique biomolecular interactions to capture and detect specific analytes on a surface. The detection versatility of biosensors has always been their key advantage and it has been demonstrated that they can detect almost any analyte such as DNA, proteins, metabolites, and even micro-organisms. However, the achievable SNR and detection DR of biosensors can be very low. This is due to the fact that the capturing processes in biosensors suffer from a significant amount of biological interference (i.e., non-specific bindings) and biochemical noise which typically necessitate the use of complex biochemical labeling processes and sophisticated detectors [1]. Hence, the main design challenge of biosensors is to increase the SNR and DR while minimizing the complexity of both the assay and the detector. Today, this is the main impediment in point-of-care (PoC) biosensors, particularly in high-performance applications such as molecular diagnostics and forensics.

In order to address this challenge, here we present a fully integrated electrochemical impedance spectroscopy (EIS) biosensor array which enables high-performance, flexible, parallel, and fully-electronic bio-molecular detection (Fig. 6.9.1). The EIS method is based on measuring the electrode-electrolyte interfacial impedance changes that occur due to analyte capturing over a wide range of frequencies [2]. The advantage of EIS over redox- [3-5], fluorescent- [6], and magnetic-based biosensing [7] is that it requires no molecular modification, label, or reporter nano-particle to detect analytes (i.e., true label-free detection [8]) while providing additional spectral information compared to capacitance-based biosensing methods [9]. EIS also acquires, in real-time, the binding kinetics which is known to be instrumental in achieving high detection DR [10]. The major challenge in designing EIS biosensors is dealing with their low transduction gain (i.e., small impedance change due to capturing) which makes the design of their detectors difficult. In this paper, we demonstrate that by leveraging the capabilities of CMOS ICs we can address this problem and build a fully-integrated EIS biosensor array with superior performance ( $10^{-9}\Omega^{-1}$  sensitivity and in excess of 90dB DR) compared to EIS stand-alone instruments. This 2mm $\times$ 2mm IC consists of 10 $\times$ 10 biosensor pixels which each include not only a bio-functionalized sensing electrode, but also the EIS detection circuitry.

The in-pixel biosensing electrodes are created by forming passivation openings on the top metal layer of the CMOS process as it is done for I/O pads. To create a universal electrode surface, we use electroless plating to deposit nickel (Ni) then gold (Au) on the exposed Al surface (Fig. 6.9.1). The Au surface is then bio-functionalized by covalently attaching a biocompatible self-assembled monolayer (SAM) which consists of linker molecules such as 11-Mercaptoundecanoic acid (11-MUA). This SAM layer can subsequently be used for the immobilization of different capturing probes such as DNA or proteins.

The architecture of the biosensor array is illustrated in Fig. 6.9.2. The objective is to measure, in real-time, the admittance of the bio-functionalized electrode-electrolyte interface,  $Y(\omega)$ , in each biosensor pixel over a wide range of frequencies (10Hz-50MHz). Our detection approach is to place a reference electrode in the solution to establish a controlled sinusoidal voltage (excitation signal),  $V_x(\omega)$ , across all electrode interfaces and measure both the amplitude and the phase of the generated current,  $I(\omega)$ , in individual pixels. By using the values of  $V_x(\omega)$  and the  $i^{\text{th}}$  pixel current,  $I_i(\omega)$ , we can then compute the  $i^{\text{th}}$  pixel interface admittance as  $Y_i(\omega) = I_i(\omega) / V_x(\omega)$ .

To measure the amplitude and phase of  $I_i(\omega)$ , we implement a direct-conversion (zero-IF) receiver operating at frequency  $\omega$  in each pixel. The operation principle in this system is similar to lock-in amplifiers [11]. This "receiver" consists of a low-noise transimpedance amplifier (TIA) and two quadrature phase mixers. The orthogonal  $I$  and  $Q$  signals are created by an on-chip digital quadrature generator using an external LO operating at  $f_{in} = 4\omega$ . The signal  $V_x(\omega)$  has adjustable amplitude (1-100mV) and is derived using the  $I$  signal and hence phase-locked to it. We also use a low-pass filter to suppress the higher-order odd harmonics of  $V_x(\omega)$  and prevent their interference with the direct-conversion detection. Each pixel has two DC outputs,  $V_I$  and  $V_Q$ , which can be sequentially scanned from array output bus. For detection, we can use the following to estimate  $Y_i(\omega)$ :

$$|Y_i(\omega)| = \frac{\sqrt{V_I^2(i) + V_Q^2(i)}}{A \cdot |V_x(\omega)|} \quad (1)$$

and

$$\angle Y_i(\omega) = \tan^{-1} \left( \frac{V_Q(i)}{V_I(i)} \right), \quad (2)$$

where  $A$  is the gain of the receive chain.

In Fig. 6.9.3, we show the pixel-level circuit topology. The low-noise TIA has a gain-booster common-gate amplifier topology where its input is directly connected to the pixel sensing electrode. The input impedance of the amplifier is kept  $<100\Omega$ , much less than electrode-electrolyte impedance (typically  $>10k\Omega$ ) for the entire operation frequency range. This is done by increasing the effective  $g_m$  of  $M_1$  using a differential amplifier in the gain-boosting circuitry. Another key function of this differential amplifier is to set the DC voltage between the sensing electrode and the reference electrode and hence control possible Faradaic processes. The current flowing through this input stage, i.e.  $I_i(\omega)$ , is mirrored by  $M_2$ ,  $M_3$ , and  $M_4$  to a set of double-balanced Gilbert-cell mixers. To minimize the input DC mismatch of the mixers, a replica of the low-noise TIA is integrated within each pixel. Also, resistors are used as the load for the mixer to minimize the output  $1/f$  noise.

In Fig. 6.9.4, we show the measured performance of the biosensor pixels. EIS requires narrowband (single-tone) detection and thus the minimum detection level (MDL) is a function of the receiver bandwidth, its noise PSD, and  $V_x(\omega)$ . On the other hand, the highest-detection level (HDL) is a function of the receiver nonlinearity. Figures 6.9.4a and 6.9.4b show the measured input-referred noise PSD (around  $\omega$ ) and the linearity of the receiver. By using these results, we have plotted the achievable detection DR for various amplitudes of  $V_x(\omega)$  in Fig. 6.9.4c. As evident, we can achieve detection DR in excess of 90dB and admittance sensitivities in the range of  $10^{-9}\Omega^{-1}$ . This level of sensitivity and DR surpasses the performance of commercially available EIS systems.

In Fig. 6.9.5, we show the measurement results of label-free detection for a variety of analytes using the CMOS EIS biosensor array in different frequency ranges. The unique impedance spectrums of DNA, BSA and the Protein G in particular, show the versatility of this system and its potential use in DNA and protein identification and detection assays. We believe that the achieved specifications of this chip (Fig. 6.9.6) in addition to the non-invasive and label-free detection capabilities of EIS are instrumental for the design of open-platform PoC biosensors, especially in applications where assay simplicity, speed, cost, and portability are imperative.

### References:

- [1] A. Hassibi, H. Vikalo and A. Hajimiri, "On Noise Processes and Limits of Performance in Biosensors," *Journal of Applied Physics*, vol. 102, iss. 1, no. 014909, Jul. 2007.
- [2] E. Katz and I. Willner, "Probing Biomolecular Interactions at Conductive and Semiconductive Surfaces by Impedance Spectroscopy: Routes to Impedimetric Immunosensors, DNA-Sensors, and Enzyme Biosensors," *Electroanalysis*, vol. 15, iss. 11, pp. 913-947, Feb. 2003.
- [3] M. Schienle *et al.*, "A Fully Electronic DNA Sensor with 128 Positions and In-pixel A/D Conversion," *IEEE J. Solid-State Circuits*, vol. 39, no. 2, pp. 2438-2445, Dec. 2004.
- [4] F. Heer, M. Keller, G. Yu, J. Janata, M. Josowicz, and A. Hierlemann, "CMOS Electro-Chemical DNA-Detection Array with On-Chip ADC," *ISSCC Dig. Tech. Papers*, pp. 168-169, Feb. 2008.
- [5] P. M. Levine, P. Gong, R. Levicky and K. Shepard, "Active CMOS Sensor array for Electrochemical Biomolecular Detection," *IEEE J. Solid-State Circuits*, vol. 43, no. 8, pp. 1859-1871, Aug. 2008.
- [6] B. Jang, P. Cao, A. Chevalier, A. Ellington, and A. Hassibi, "A CMOS Fluorescence-based Biosensor Microarray," *ISSCC Dig. Tech. Papers*, pp. 436-437, Feb. 2009.
- [7] H. Wang, Y. Chen, A. Hassibi, A. Scherer, and A. Hajimiri, "A Frequency-Shift CMOS Magnetic Biosensor Array with Single-bead Sensitivity and No External Magnet," *ISSCC Dig. Tech. Papers*, pp. 438-439, Feb. 2009.
- [8] J. S. Daniels and N. Pourmand, "Label-Free Impedance Biosensors: Opportunities and Challenges," *Electroanalysis*, vol. 19, iss. 12, pp. 1239 - 1257, May 2007.
- [9] C. S. D. Esposti *et al.*, "Fully Electronic CMOS DNA Detection Array Based on Capacitance Measurement with On-Chip Analog-to-Digital Conversion," *ISSCC Dig. Tech. Papers*, pp. 48-49, Feb. 2006.
- [10] A. Hassibi, H. Vikalo, J. L. Riechmann and B. Hassibi, "Real-time DNA Microarray Analysis," *Nucleic Acids Research*, doi:10.1093/nar/gkp675, Sep. 2009.
- [11] G. Ferri, P. De Laurentiis, A. D'Amico, and C. Di Natale, "A Low-voltage Integrated CMOS Analog Lock-in Amplifier Prototype for LAPS Applications," *Sensors and Actuators A*, vol. 92, pp. 263-272, Jan. 2001.

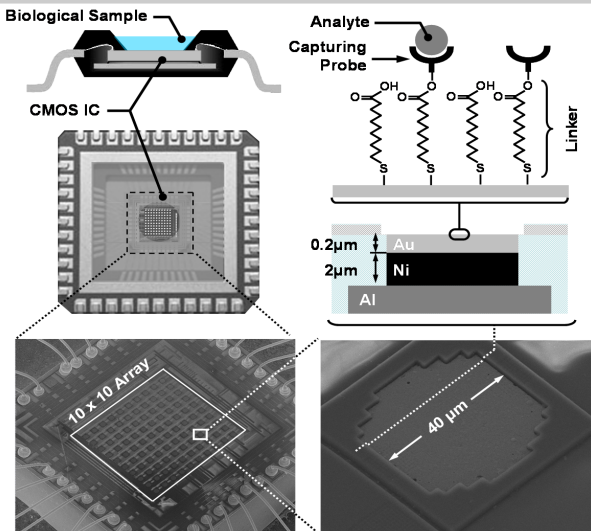


Figure 6.9.1: Electrochemical Impedance Spectroscopy (EIS) biosensor 10x10 array.

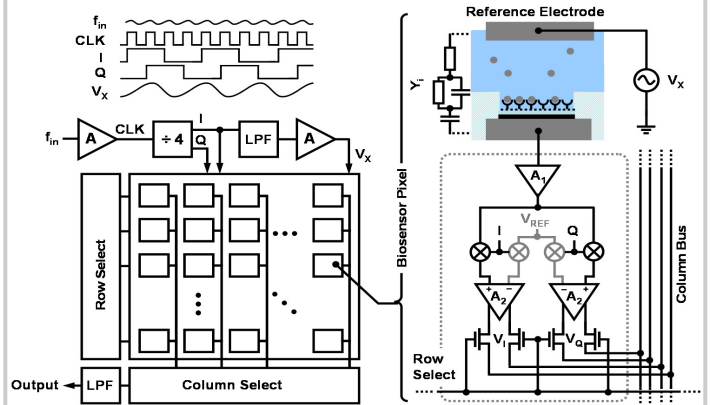


Figure 6.9.2: Architecture of the EIS biosensor array and the pixel.

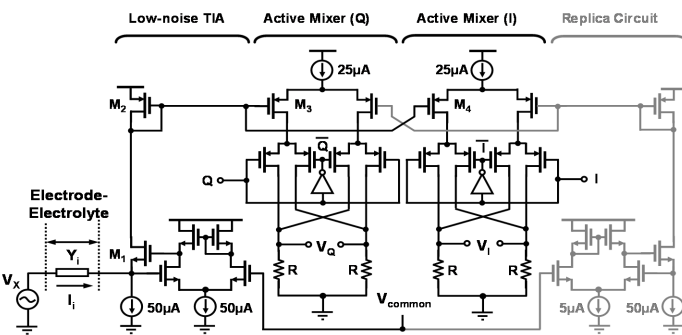


Figure 6.9.3: Circuit topology of the pixel.

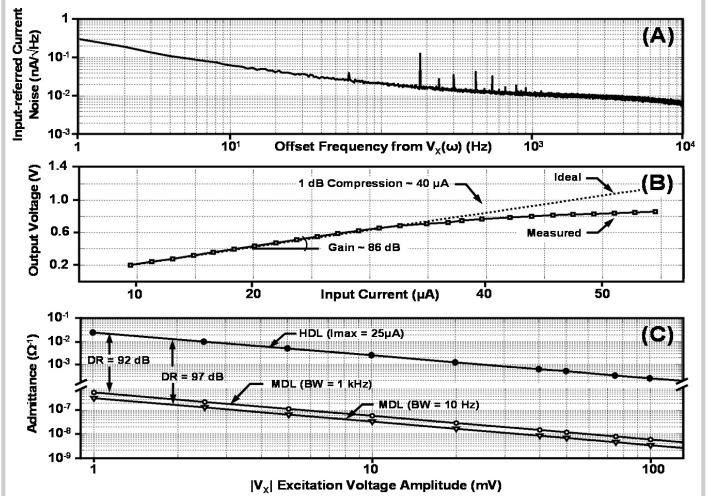


Figure 6.9.4: (A) Input-referred current noise, (B) linearity curve, and (C) admittance detection ranges.

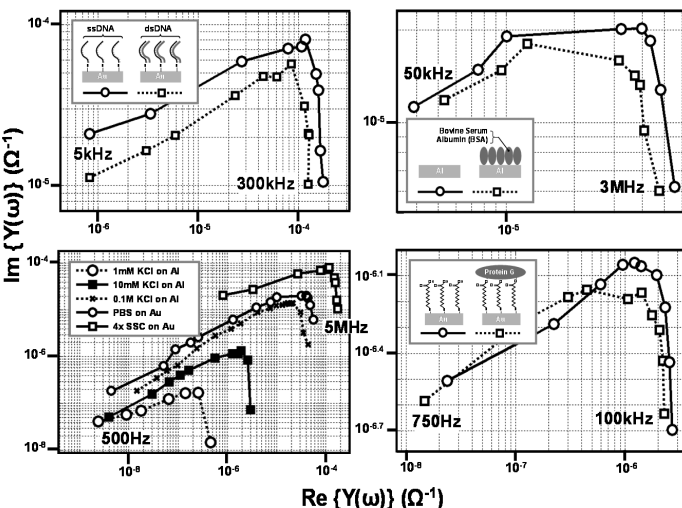


Figure 6.9.5: Impedance spectrums (real and of imaginary part of electrode-electrolyte admittance) for various buffers and DNA and protein assays.

Chip	
Technology	0.35μm CMOS, 4 metal layers, 3.3V supply
Die size	2mm x 2mm (1.2mm x 1.2mm active area)
Power consumption	84.8mW (100kHz), 104.6mW (50MHz)
Inputs	Analogue: $V_{common}$ , $V_{bias}$ , $f_{in}$ Digital: Decoder_In [0..7], Reset
Outputs	Analogue: $V_i$ , $V_r$ , $V_{Q^+}$ , $V_{Q^-}$ Digital: I, Q
EIS Biosensor Array	
Array size	10 x 10
Spectroscopy frequency range	DC - 50MHz
Scan rate	0.55 min <sup>-1</sup> (BW = 10Hz)
Pixel Specifications	
Pixel size	100μm x 100μm
Electrode	40μm x 40μm
Electrode surface	Al/1% Si, Au
Detector input impedance	96 Ω    122 fF*
Detector transimpedance gain	86 dB (σ = 0.48dB)
1 dB compression point	41 μA
Current Sensitivity (SNR = 1)	330 pA (BW = 10Hz)
Admittance MDL (SNR = 1)	3.3 x 10 <sup>-9</sup> Ω <sup>-1</sup> (BW = 10Hz,  V <sub>x</sub>   = 100mV)
Admittance HDL	250 x 10 <sup>-6</sup> Ω <sup>-1</sup> ( V <sub>x</sub>   = 100mV)
Dynamic range (DR)	97 dB (BW = 10Hz)

Figure 6.9.6: Measured performance summary (\* obtained from simulation).

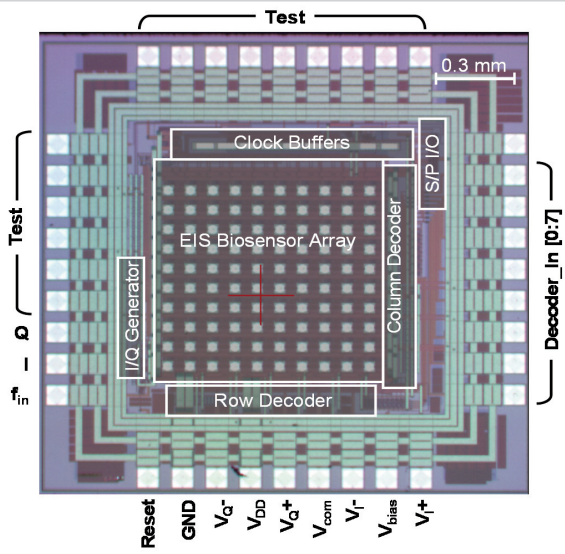


Figure 6.9.7: Chip micrograph.